

**CIRCUIT CAD AND MODELING
THROUGH SPACE MAPPING**

J.W. Bandler and J.E. Rayas-Sánchez

SOS-99-7-Vb

March 1999

(Revised June 1999)

© J.W. Bandler and J.E. Rayas-Sánchez 1999

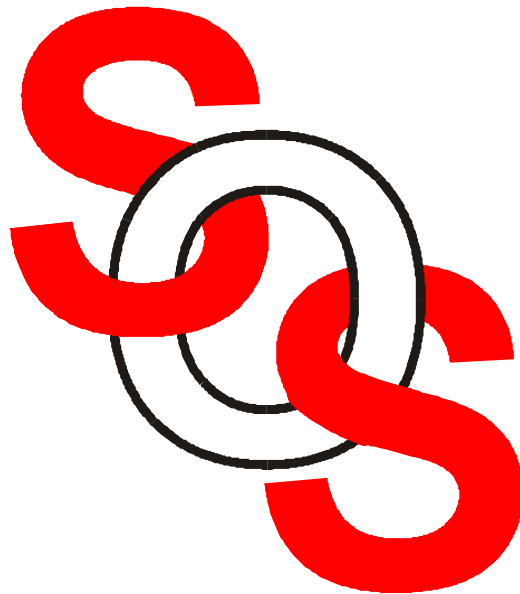
No part of this document may be copied, translated, transcribed or entered in any form into any machine without written permission. Address enquiries in this regard to Dr. J.W. Bandler. Excerpts may be quoted for scholarly purposes with full acknowledgement of source. This document may not be lent or circulated without this title page and its original cover.

CIRCUIT CAD AND MODELING THROUGH SPACE MAPPING

J.W. Bandler and J.E. Rayas-Sánchez

Simulation Optimization Systems Research Laboratory
and Department of Electrical and Computer Engineering
McMaster University, Hamilton, Canada L8S 4K1

bandler@mcmaster.ca
www.sos.mcmaster.ca



presented at

WORKSHOP ON NOVEL METHODOLOGIES FOR DEVICE MODELING AND CIRCUIT CAD

1999 IEEE MTT-S Int. Microwave Symposium, Anaheim, CA, June 13, 1999



CIRCUIT CAD AND MODELING THROUGH SPACE MAPPING

J.W. Bandler and J.E. Rayas-Sánchez

Simulation Optimization Systems Research Laboratory
and Department of Electrical and Computer Engineering
McMaster University, Hamilton, Canada L8S 4K1

bandler@mcmaster.ca
www.sos.mcmaster.ca

Abstract

We review the Space Mapping (SM) approach to circuit design and discuss modeling of microwave circuits using Artificial Neural Networks (ANN). We show that SM and ANN methodologies can be combined into a powerful design framework. SM based neuromodels decrease the cost of training, improve generalization ability and reduce the complexity of the ANN topology with respect to the classical neuromodeling approach. We present and illustrate a variety of possible SM based neuromodels, including SMN, FDSMN and FSMN. We contrast SM based neuromodeling with the classical neuromodeling approach as well as with other state-of-the-art neuromodeling techniques. The SM based neuromodeling techniques are illustrated by a microstrip line and a microstrip right angle bend.



Space Mapping Optimization

(Bandler et al., 1994-)

Aggressive Space Mapping (ASM) has been applied to design examples exploiting the EM simulators

Sonnet's *em*

Ansoft HFSS

HP HFSS

coarse models exploit coarse grid EM models or circuit-theoretic/analytical models

coarse models, decomposed into subnetworks, can even consist of a mixture of EM based subnetworks and empirical elements connected through circuit theory

new ASM algorithms TRASM (*Bakr et al., 1998*), HASM (*Bakr et al., 1999*) have been proposed



Space Mapping Based Artificial Neural Network (ANN) Modeling

(Bandler, Ismail, Rayas-Sánchez and Zhang, 1999)

Artificial Neural Networks can model high-dimensional and highly nonlinear problems *(White et al., 1992)*

ANN models are computationally efficient and can be more accurate than empirical models

ANNs are suitable models for microwave circuit optimization and statistical design *(Zaabab, Zhang and Nakhla, 1995, Gupta et al., 1996, Burrascano and Mongiardo, 1998, 1999)*

ANN modeling of microwave circuits based on Space Mapping technology are exploited for the first time *(Bandler et al., 1999)*

this takes advantage of the vast set of empirical models already available



Novel Applications of Space Mapping Technology

(Bandler et al., 1999)

we illustrate several new techniques to generate SM based neuromodels

Space Mapped Neuromodeling (SMN)

Frequency-Dependent Space Mapped Neuromodeling (FDSMN)

Frequency Space Mapped Neuromodeling (FSMN)

these techniques

- exploit the vast set of empirical models already available

- decrease the fine model evaluations needed for training

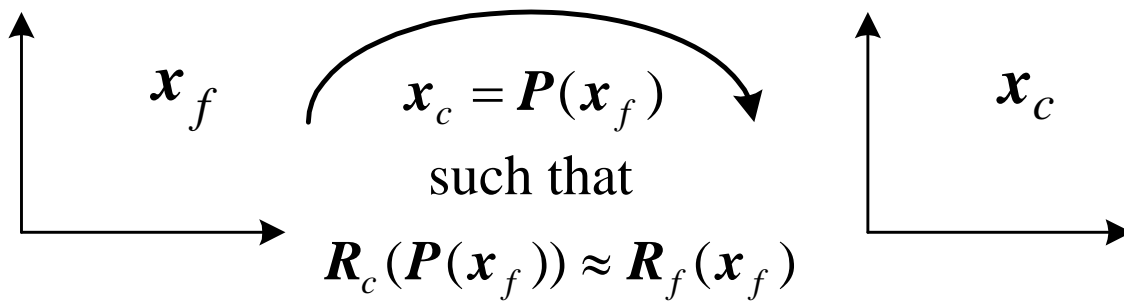
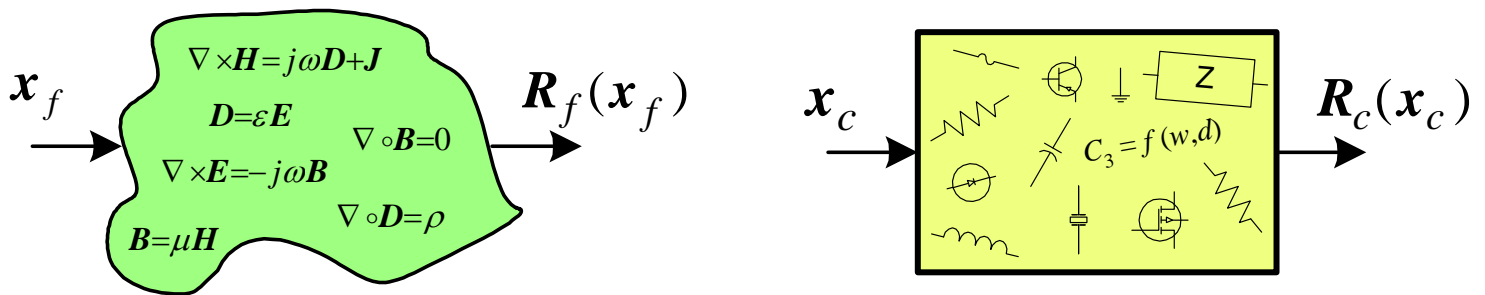
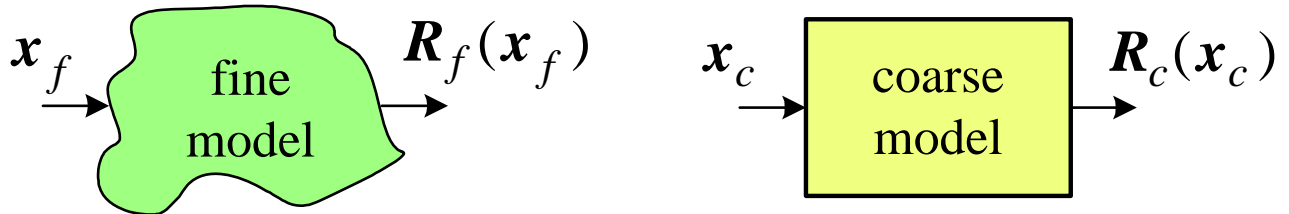
- improve generalization ability

- reduce complexity of the ANN topology

 - w.r.t. the classical neuromodeling approach

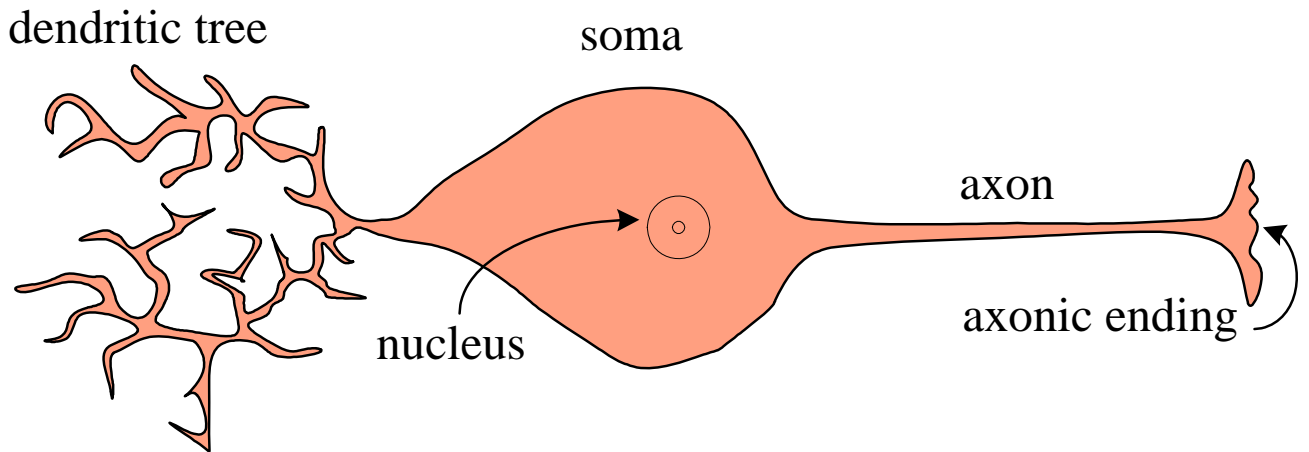


The Aim of Space Mapping



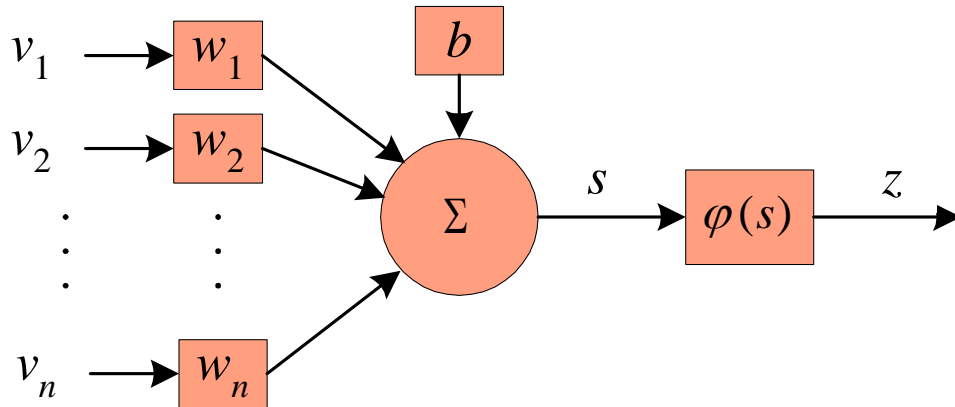


Biological Neuron
(Kartalopoulos, 1996)





Basic Model of a Neuron



$$\mathbf{v} = \begin{bmatrix} v_1 \\ v_2 \\ \vdots \\ v_n \end{bmatrix} \quad \text{vector of inputs:} \\ \text{signals from other} \\ \text{neurons}$$

$$\mathbf{w} = \begin{bmatrix} w_1 \\ w_2 \\ \vdots \\ w_n \end{bmatrix} \quad \text{vector of weights:} \\ \text{represent} \\ \text{corresponding} \\ \text{synapse strength}$$

b is the bias or offset term

$s = b + \mathbf{v}^T \mathbf{w}$ is the activation signal

$z = \varphi(s)$ is the output signal

if a sigmoid activation function is used

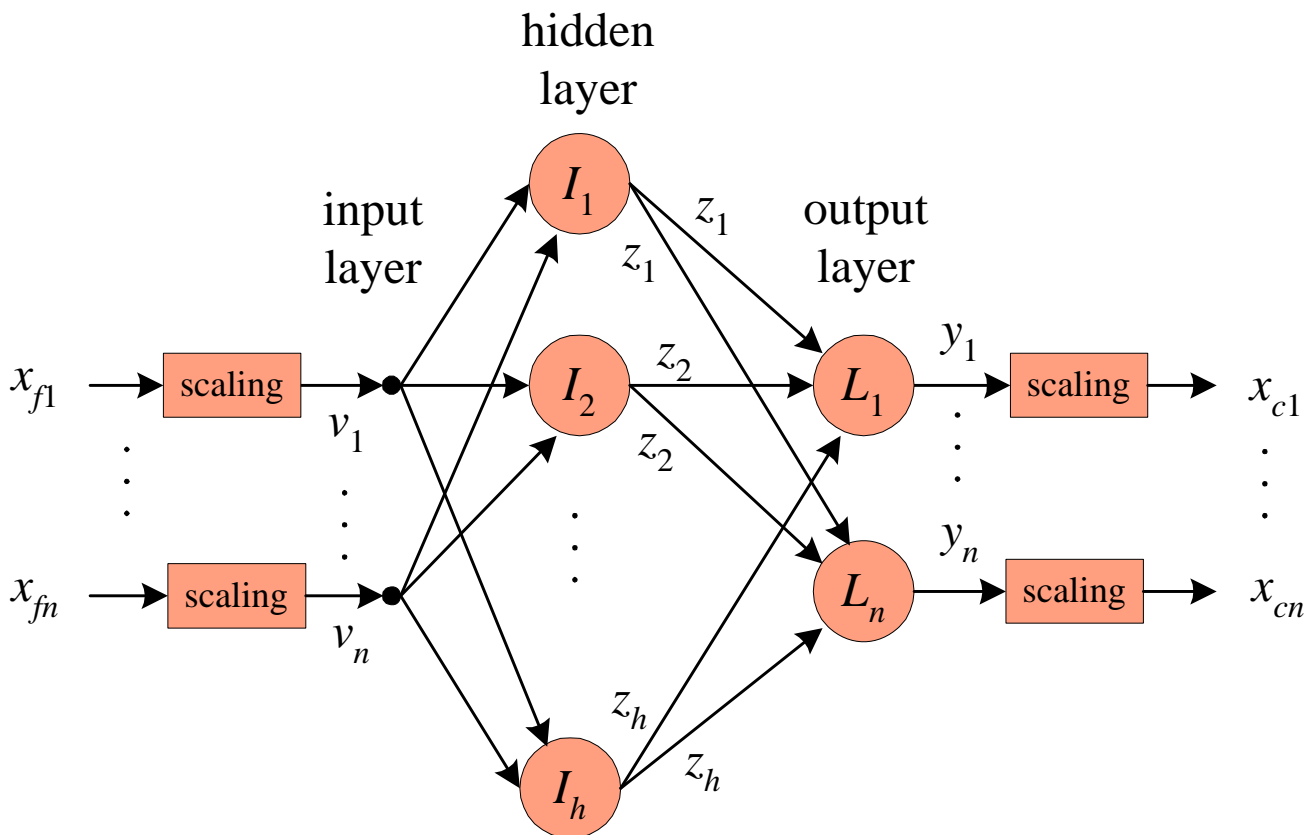
$$z = \varphi(s) = \frac{1}{1 + e^{-s}}$$



Neural Space Mapping



using a three layer perceptron (3LP)





Three Layer Perceptron (3LP)

$\mathbf{x}_f = [x_{f1} \quad x_{f2} \quad \cdots \quad x_{fn}]^T$ are n input physical parameters

$\mathbf{v} = [v_1 \quad v_2 \quad \cdots \quad v_n]^T$ are input signals after scaling

$\mathbf{z} = [z_1 \quad z_2 \quad \cdots \quad z_h]^T$ are signals from the h hidden neurons

$\mathbf{y} = [y_1 \quad y_2 \quad \cdots \quad y_n]^T$ are n output signals before scaling

$\mathbf{x}_c = [x_{c1} \quad x_{c2} \quad \cdots \quad x_{cn}]^T$ are the neuromapping outputs

to control the relative importance of the input parameters and define a suitable dynamic range, scaling can be used

$$v_i = -1 + \frac{2(x_{fi} - x_{fi \min})}{(x_{fi \max} - x_{fi \min})}, \quad i = 1, 2, \dots, n$$



Three Layer Perceptron (continued)

the hidden layer signals are calculated by

$$z_i = \varphi(b_i^h + \mathbf{v}^T \mathbf{w}_i^h), \quad i = 1, 2, \dots, h$$

\mathbf{w}_i^h are the vectors of synaptic weights of the hidden neurons

$$\mathbf{w}_i^h = [w_{i1}^h \quad w_{i2}^h \quad \dots \quad w_{in}^h]^T, \quad i = 1, 2, \dots, h$$

\mathbf{b}^h is the vector of bias elements for the hidden neurons

$$\mathbf{b}^h = [b_1^h \quad b_2^h \quad \dots \quad b_h^h]^T$$

the output layer signals are given by

$$y_i = b_i^o + \mathbf{z}^T \mathbf{w}_i^o, \quad i = 1, 2, \dots, n$$

\mathbf{w}_i^o are the vectors of synaptic weights of the output neurons

$$\mathbf{w}_i^o = [w_{i1}^o \quad w_{i2}^o \quad \dots \quad w_{ih}^o]^T, \quad i = 1, 2, \dots, n$$

\mathbf{b}^o is the vector of bias elements for the output neurons

$$\mathbf{b}^o = [b_1^o \quad b_2^o \quad \dots \quad b_n^o]^T$$



Three Layer Perceptron (continued)

to provide a scaling for the output signals equivalent to the one used in the input

$$x_{ci} = x_{fi \min} + \frac{1}{2}(y_i + 1)(x_{fi \max} - x_{fi \min}), \quad i = 1, 2, \dots, n$$

all internal parameters of the ANN can be grouped as

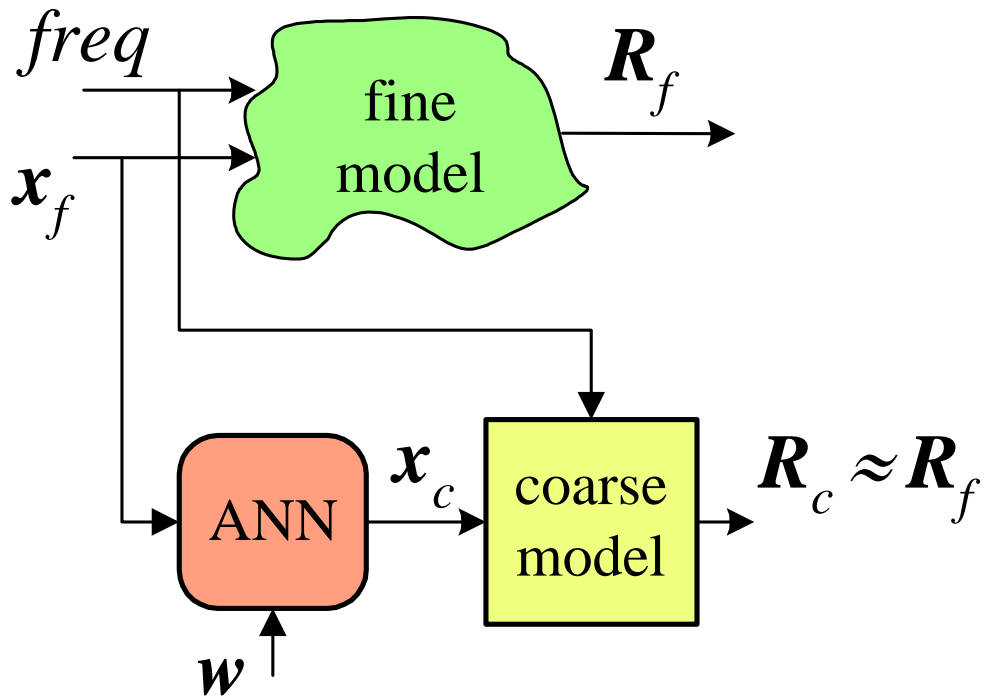
$$\mathbf{w} = [(\mathbf{b}^h)^T \quad (\mathbf{w}_1^h)^T \quad \dots \quad (\mathbf{w}_h^h)^T \quad (\mathbf{b}^o)^T \quad (\mathbf{w}_1^o)^T \quad \dots \quad (\mathbf{w}_n^o)^T]^T$$

the number of optimization variables for a three-layer perceptron with n inputs, n outputs and h hidden neurons is

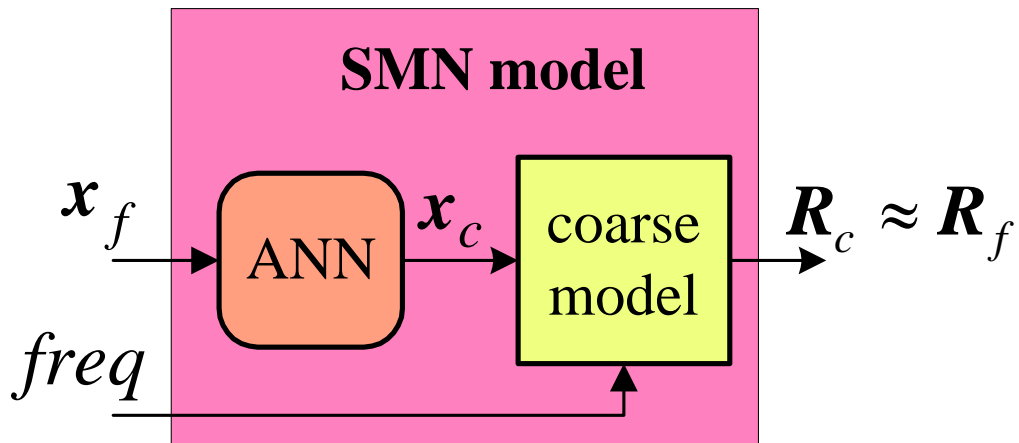
$$n(2h+1)+h$$



Space Mapped Neuromodeling (SMN) Concept



once the ANN is trained



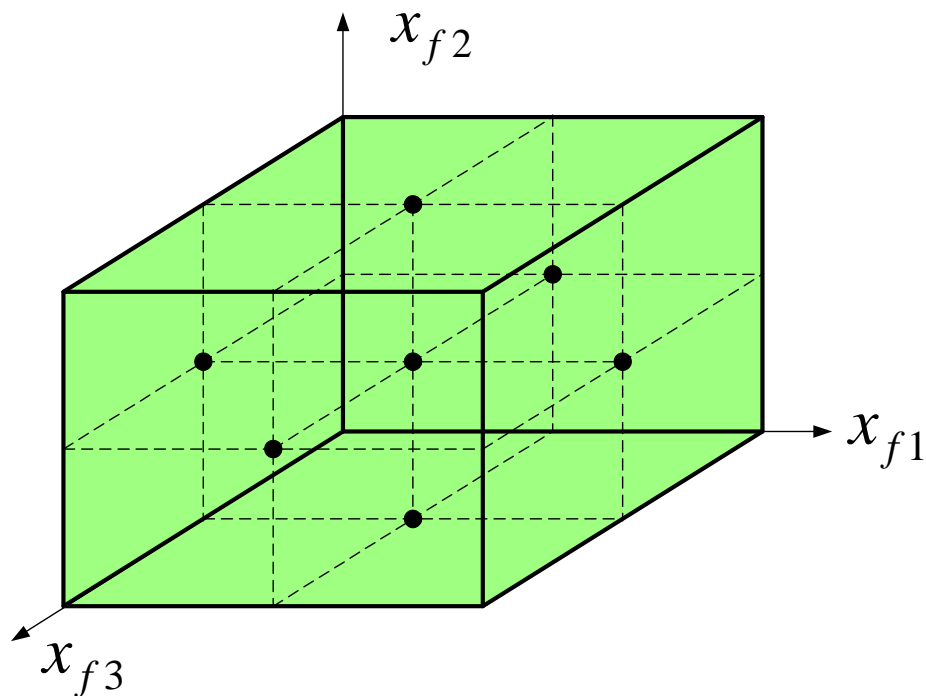


Three-dimensional Star Distribution for the Learning Base Points

(Bandler et al., 1989)

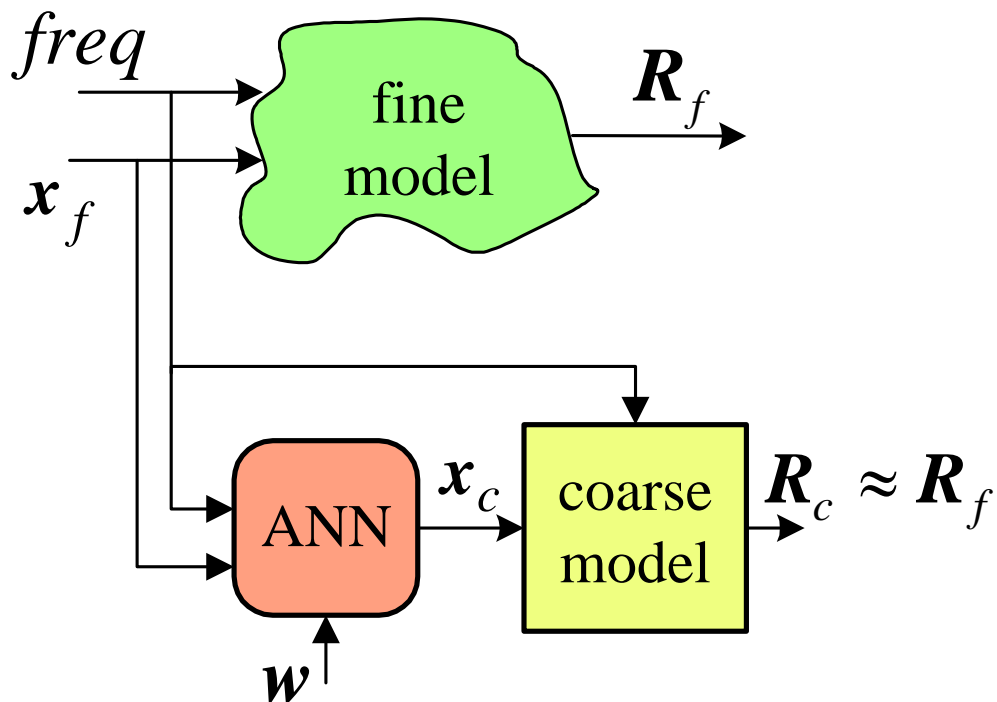
to keep a reduced set of learning data samples, we consider an n -dimensional star distribution for the base learning points

the number of learning base points for a microwave circuit with n design parameters is $B_p = 2n + 1$

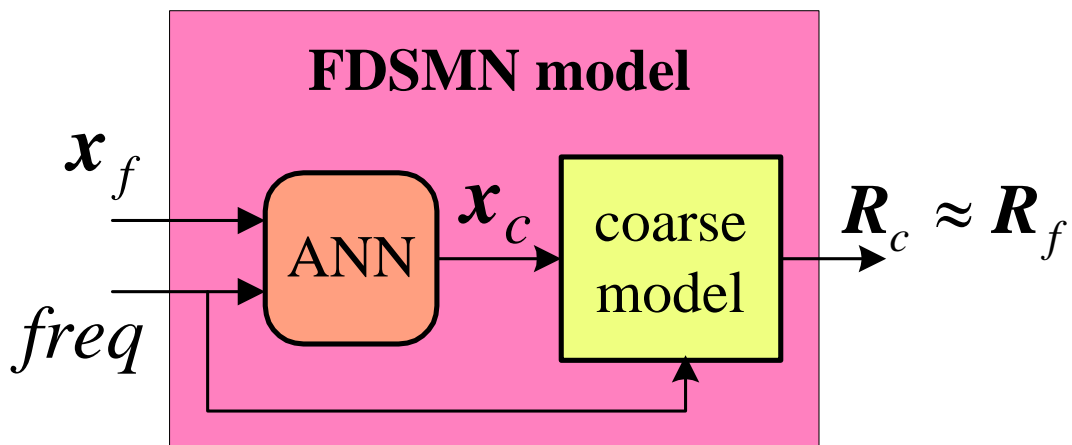




Frequency-Dependent Space Mapped Neuromodeling (FDSMN) Concept

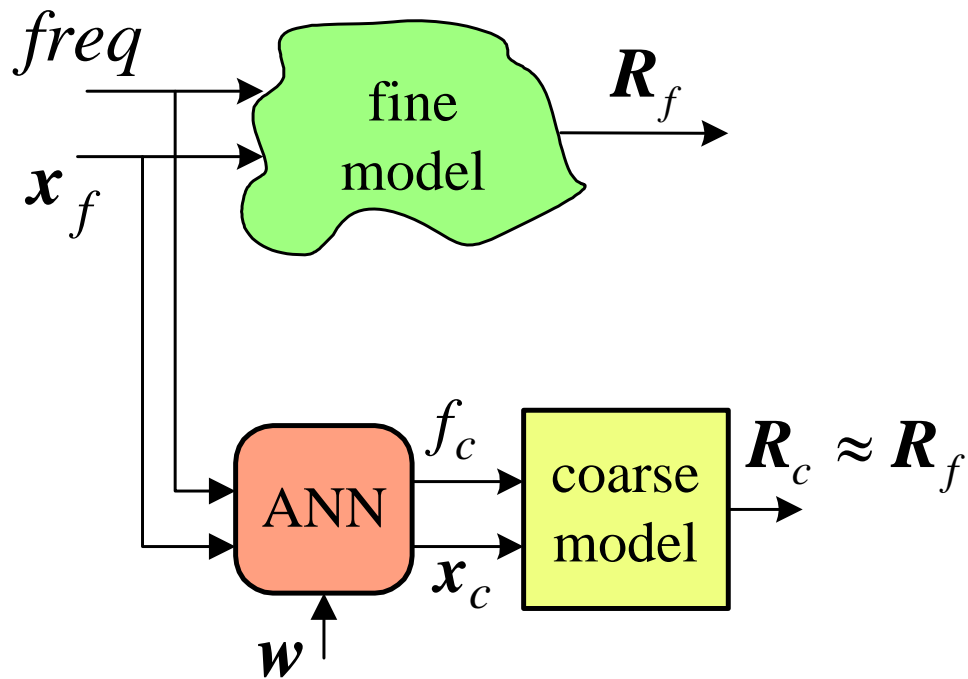


once the ANN is trained

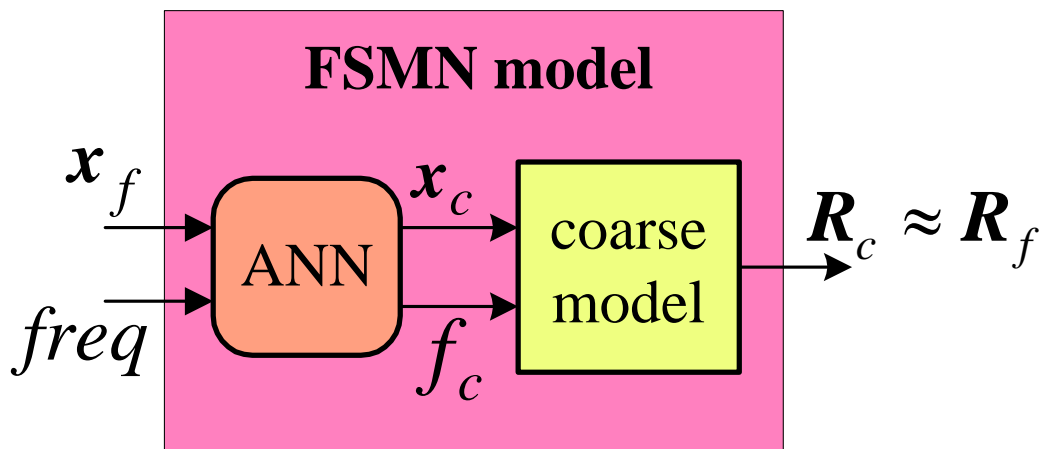




Frequency Space Mapped Neuromodeling (FSMN) Concept



once the ANN is trained





Training the ANN

the neuromapping can be found by solving the optimization problem

$$\min_w \left\| [e_1^T \quad e_2^T \quad \cdots \quad e_l^T]^T \right\|$$

w contains the internal parameters of the ANN (weights, bias, etc.) selected as optimization variables

l is the total number of learning samples

e_k is the error vector given by

for SMN

$$e_k = \mathbf{R}_f(\mathbf{x}_{f_i}, freq_j) - \mathbf{R}_c(\mathbf{x}_c, freq_j)$$

$$\mathbf{x}_c = \mathbf{P}(\mathbf{x}_{f_i})$$

for FDSMN

$$e_k = \mathbf{R}_f(\mathbf{x}_{f_i}, freq_j) - \mathbf{R}_c(\mathbf{x}_c, freq_j)$$

$$\mathbf{x}_c = \mathbf{P}(\mathbf{x}_{f_i}, freq_j)$$



Training the ANN (continued)

for FSMN

$$\mathbf{e}_k = \mathbf{R}_f(\mathbf{x}_{f_i}, freq_j) - \mathbf{R}_c(\mathbf{x}_c, f_c)$$
$$\begin{bmatrix} \mathbf{x}_c \\ f_c \end{bmatrix} = \mathbf{P}(\mathbf{x}_{f_i}, freq_j)$$

with

$$i = 1, \dots, B_p$$

$$j = 1, \dots, F_p$$

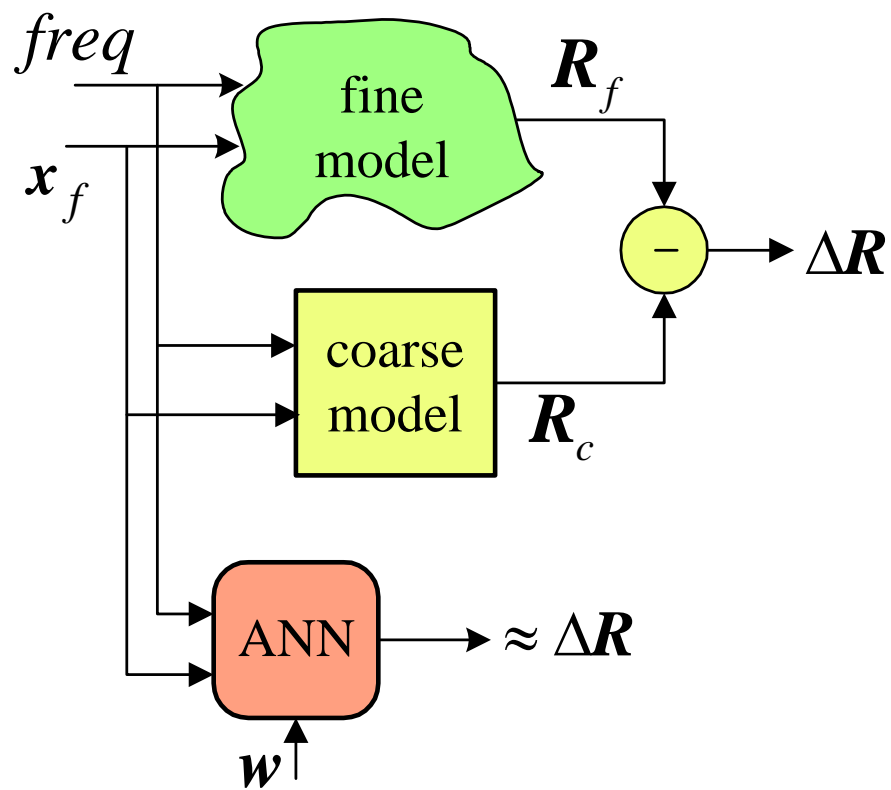
$$k = j + F_p(i - 1)$$



EM-ANN Neuromodeling Concept

(Gupta et al., 1996)

an interpretation using our notation

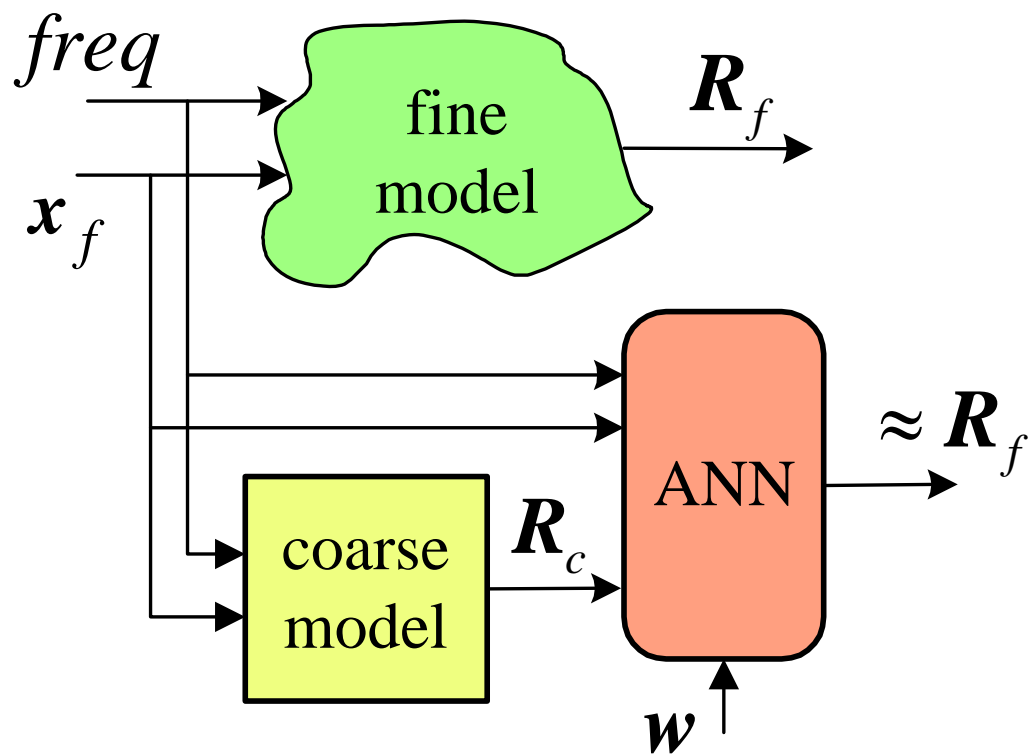




PKI Neuromodeling Concept

(Gupta et al., 1996)

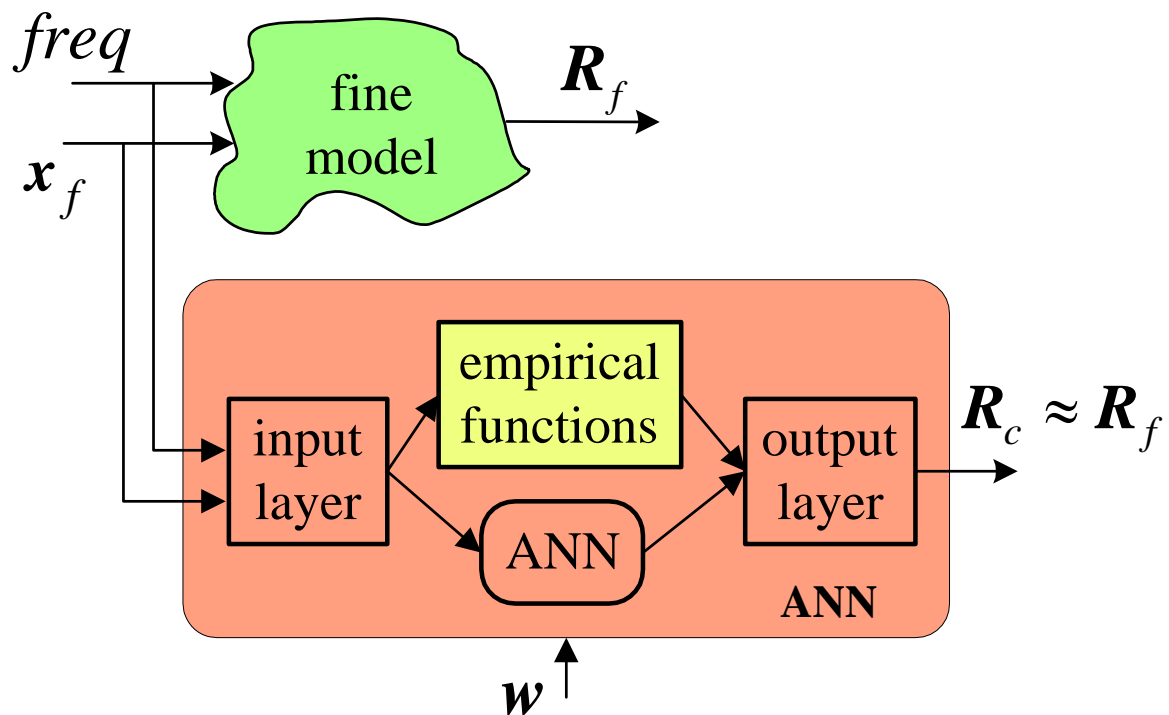
an interpretation using our notation



KBNN Neuromodeling Concept

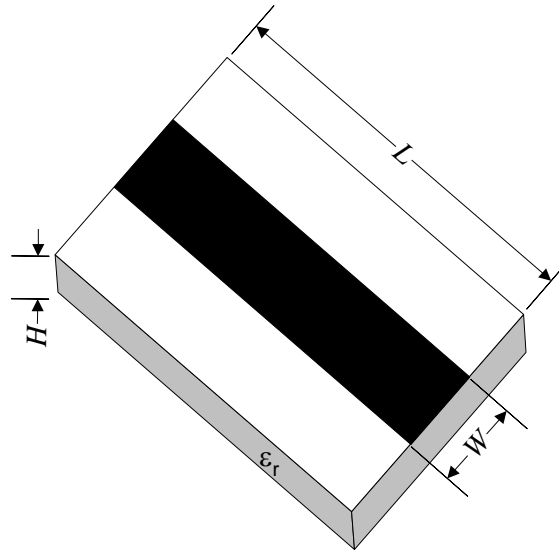
(Zhang et al., 1997)

an interpretation using our notation





Microstrip Line with High Dielectric Constant



region of interest

$$5\text{mil} \leq W \leq 9\text{mil}$$

$$15\text{mil} \leq H \leq 25\text{mil}$$

$$40\text{mil} \leq L \leq 60\text{mil}$$

$$20 \leq \epsilon_r \leq 25$$

$$27\text{GHz} \leq \text{freq} \leq 30\text{GHz}.$$

“coarse” model: Pozar’s formulas (*Pozar, 1998*)

“fine” model: Sonnet’s *em*TM

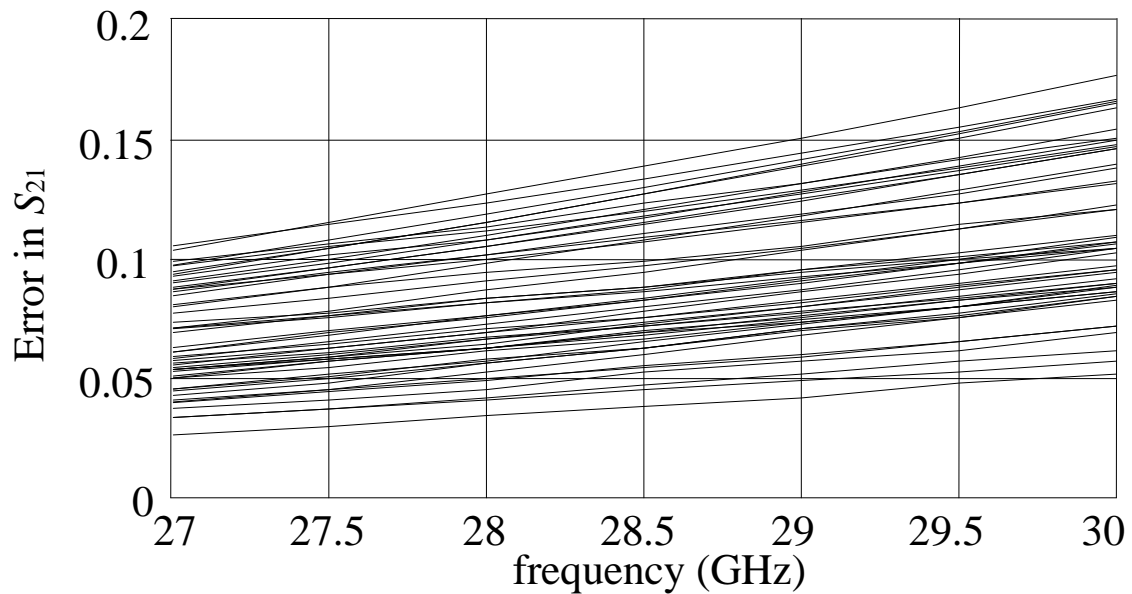
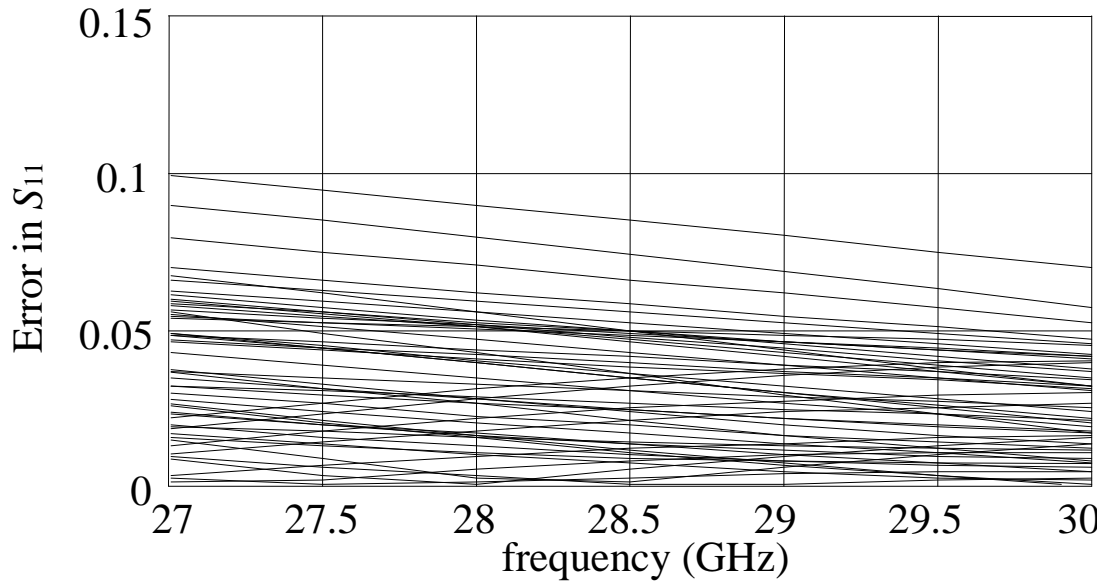
learning set: 9 base points with “star” distribution

testing set: 50 random base points in the region of interest



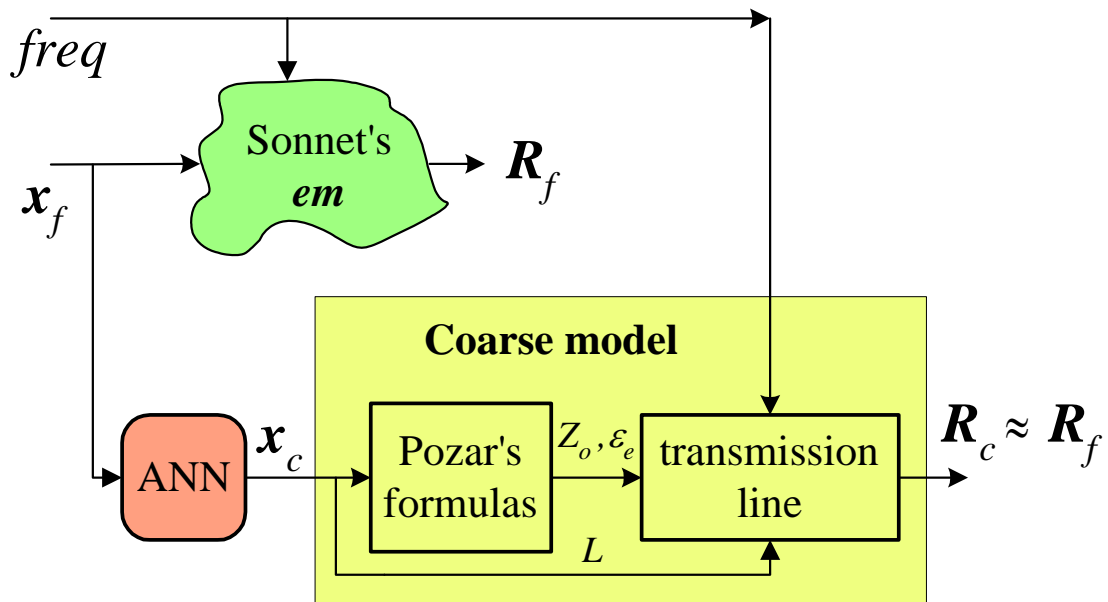
Microstrip Line Response Errors

comparison before neuromodeling between *em*TM and Pozar's model at 50 random test points





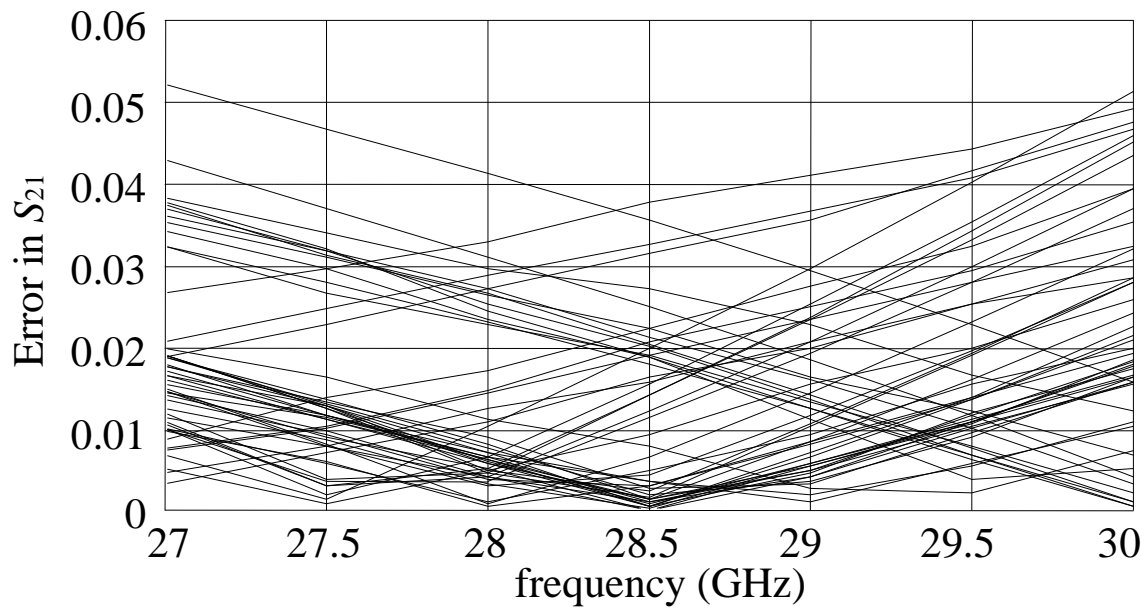
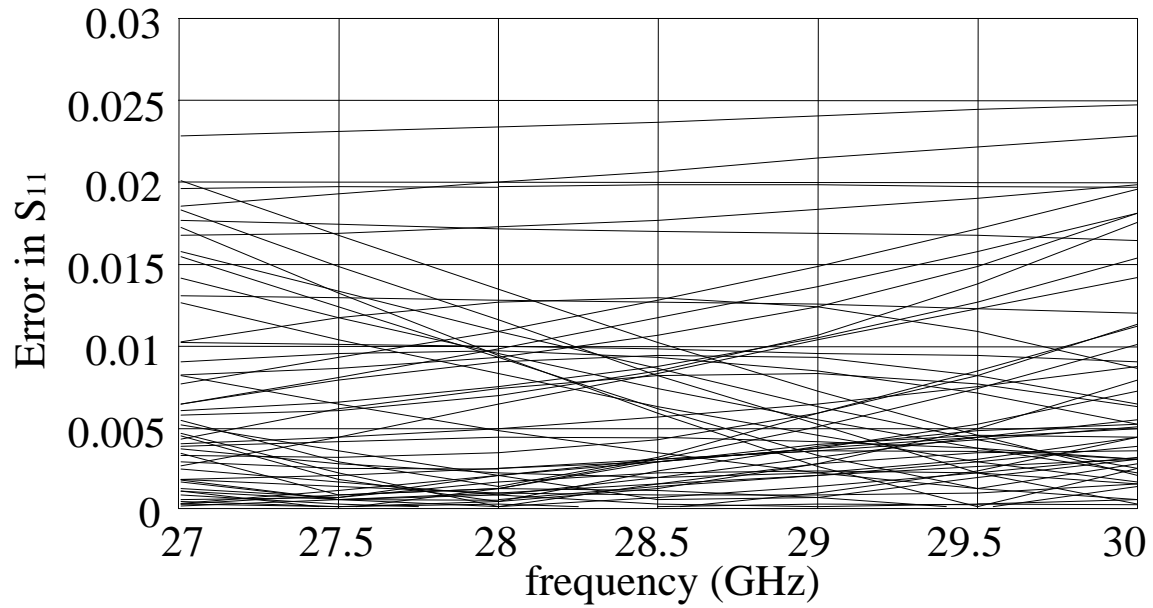
SMN Model for the Microstrip Line (3LP:4-3-4)





SMN Model Results for the Microstrip Line

comparison between *em*TM and the SMN model





SMN Model for the Microstrip Line Implemented in OSA90

Expression

```
! w : Width of the flat conductor in the PCB (in mils)
! h : Thickness of the PWB laminate (in mils)
! l : Length of the flat conductors (in mils)
! epsr : Dielectric constant of the PWB laminate
! Xf[i]= [w(i) h(i) l(i) epsr(i)]
i: 1;! Index for the training/test points
end
```

Model

```
#include "mcs1_hepsr.inc";
! SONNET'S MODEL:
mcs1_hepsr @f1 @f2 0
l=(Xf[i,3]*1mil) w=(Xf[i,1]*1mil)
h=(Xf[i,2]*1mil) epsr=(Xf[i,4]);
ports @f1 0 @f2 0 ;! Ports 1-2 for Sonnet's model

! Neuromapping (3LP: 4-3-4)
! .....

! input scaling
v1=-1+2*(Xf[i,1]-Xf1_min) / (Xf1_max - Xf1_min);
v2=-1+2*(Xf[i,2]-Xf2_min) / (Xf2_max - Xf2_min);
v3=-1+2*(Xf[i,3]-Xf3_min) / (Xf3_max - Xf3_min);
v4=-1+2*(Xf[i,4]-Xf4_min) / (Xf4_max - Xf4_min);

! vectors of synaptic weights of the hidden neurons : wh
wh1[4]: [?0.0997064? ?0.00926408? ?-0.0010517? ?0.00555616?];
wh2[4]: [? -0.0254024? ?0.100381? ?0.00506993? ?-0.0277744?];
wh3[4]: [? -0.00263021? ?0.00403475? ?0.152244? ?0.0449023?];

! vector of bias elements for the hidden neurons : bh
bh[3]: [?0.0379664? ?-0.0373888? ?0.016498?];

! hidden layer
z1 = tanh(bh[1]+v1*wh1[1]+v2*wh1[2]+v3*wh1[3]+v4*wh1[4]);
z2 = tanh(bh[2]+v1*wh2[1]+v2*wh2[2]+v3*wh2[3]+v4*wh2[4]);
z3 = tanh(bh[3]+v1*wh3[1]+v2*wh3[2]+v3*wh3[3]+v4*wh3[4]);

! vectors of synaptic weights of the output neurons : wo
wo1[3]: [?9.97323? ?8.37909e-005? ?6.37812e-006?];
wo2[3]: [? -0.000228351? ?10.0461? ?-7.25383e-005?];
wo3[3]: [?0.0112826? ?-0.0014412? ?6.85617?];
wo4[3]: [?0.00258169? ?0.000209437? ?-0.00683818?];
! vector of bias elements for the output neurons : bo
bo[4]: [?0.00394671? ?-0.00393648? ?0.0121073? ?-0.01383?];
```



```
! output layer
y1 = bo [1]+z1*wo1 [1]+z2*wo1 [2]+z3*wo1 [3];
y2 = bo [2]+z1*wo2 [1]+z2*wo2 [2]+z3*wo2 [3];
y3 = bo [3]+z1*wo3 [1]+z2*wo3 [2]+z3*wo3 [3];
y4 = bo [4]+z1*wo4 [1]+z2*wo4 [2]+z3*wo4 [3];

! output scaling
Xc1 = Xf1_min + 0.5*(y1+1)*(Xf1_max - Xf1_min);
Xc2 = Xf2_min + 0.5*(y2+1)*(Xf2_max - Xf2_min);
Xc3 = Xf3_min + 0.5*(y3+1)*(Xf3_max - Xf3_min);
Xc4 = Xf4_min + 0.5*(y4+1)*(Xf4_max - Xf4_min);

! POZAR'S MODEL (TRANSMISSION LINE)

epse=(Xc4+1)/2+(Xc4-1)/(2 *sqrt (1+12*Xc2/Xc1));
Zo= if ((Xc1/Xc2)<1)
    (60/sqrt(epse) * log (8*Xc2/Xc1+Xc1/(4*Xc2)))
    else
    (120*pi/(sqrt (epse)*(Xc1/Xc2+1.393+0.667*log (Xc1/Xc2+1.444))));
TRL @c1 @c2 Z=Zo L=(Xc3*1mil) K=epse F=FREQ;
ports @c1 0 @c2 0 ;! Ports 3-4 for Pozar's model
CIRCUIT;
end

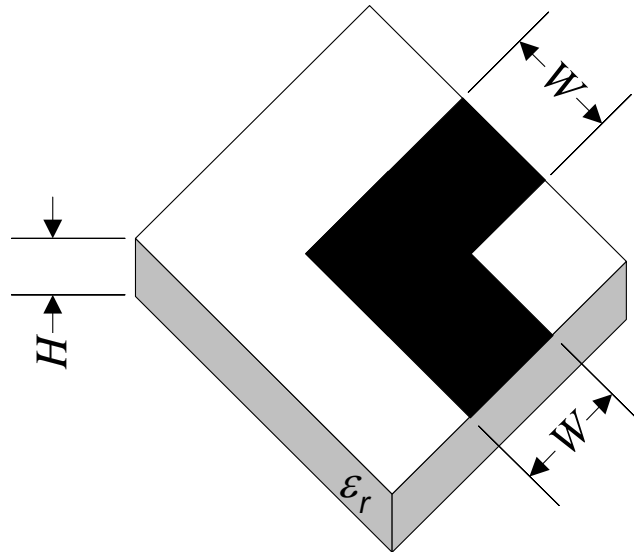
Sweep
AC: i: from 1 to N step 1
    FREQ: from Freq_min to Freq_max step=Freq_step
    "rS11 (Sonnet)", "iS11 (Sonnet)", "rS21 (Sonnet)", "iS21 (Sonnet)"
    "rS11 (SMN)", "iS11 (SMN)", "rS21 (SMN)", "iS21 (SMN)"
end

Specification
AC: i: from 1 to NL step 1
    FREQ: from Freq_min to Freq_max step=Freq_step
        "rS11 (SMN)" = "rS11 (Sonnet)"
        "iS11 (SMN)" = "iS11 (Sonnet)"
        "rS21 (SMN)" = "rS21 (Sonnet)"
        "iS21 (SMN)" = "iS21 (Sonnet)"
end

Control
Perturbation_Scale=1.0e-4;
Disable_Adjoint;
Allow_Neg_Parameters;
Optimizer=Huber;
N_iteations=100;
Display_N_digits=6;
Accuracy=1.0e-5;
Huber_threshold=0.15;
end
```



Microstrip Right Angle Bend



region of interest

$$20\text{mil} \leq W \leq 30\text{mil}$$

$$8\text{mil} \leq H \leq 16\text{mil}$$

$$8 \leq \epsilon_r \leq 10$$

$$1\text{GHz} \leq \text{freq} \leq 41\text{GHz}$$

“coarse” model: Gupta model (*Gupta, Garg and Bahl, 1979*)

“fine” model: Sonnet’s *em*TM

learning set: 7 base points with “star” distribution

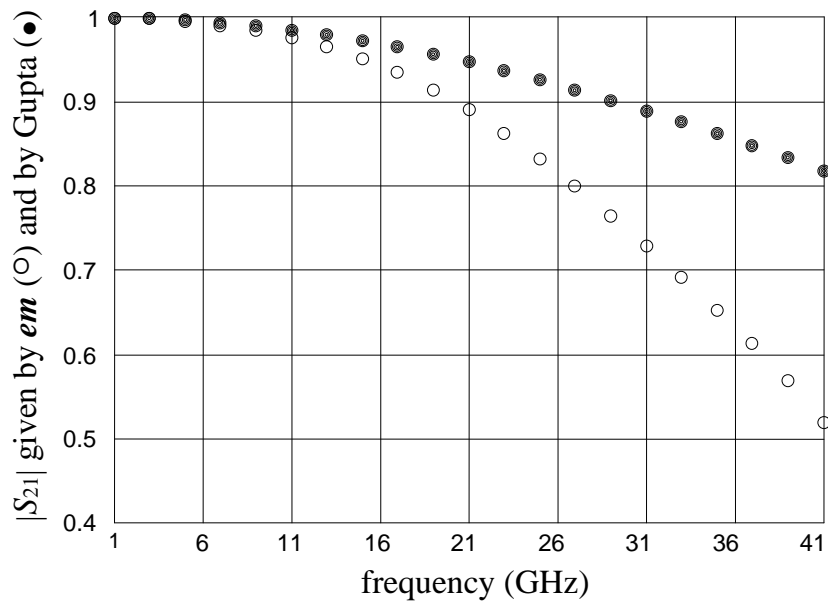
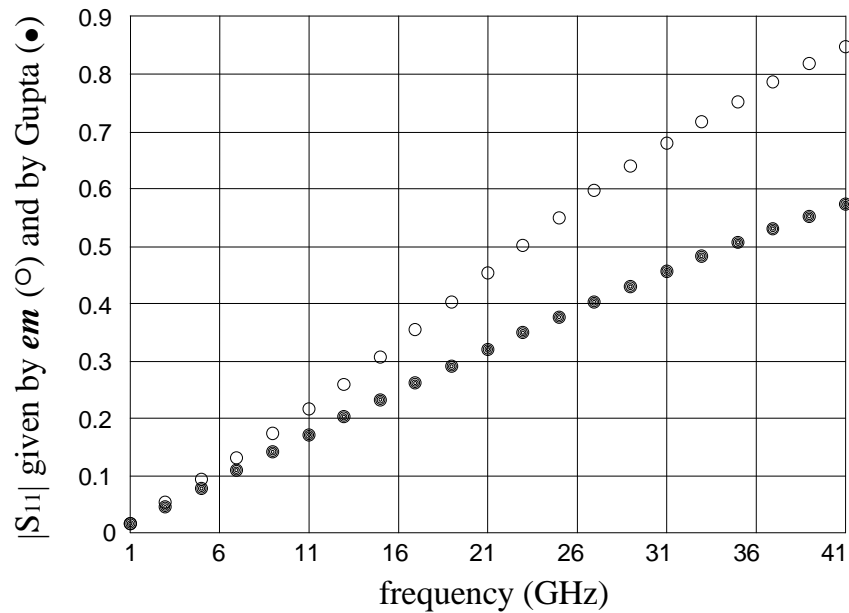
testing set: 50 random base points in the region of interest



Microstrip Right Angle Bend Responses

typical responses before neuromodeling

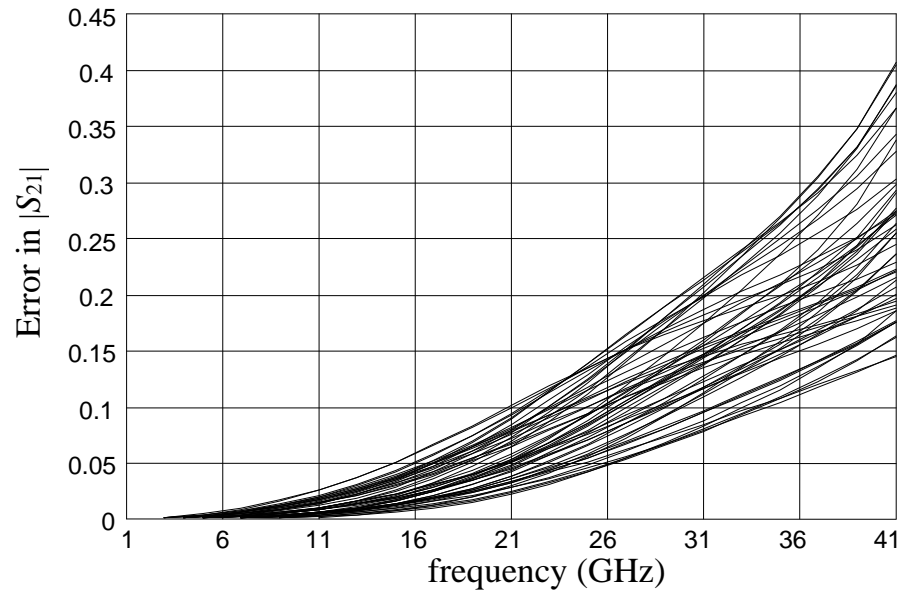
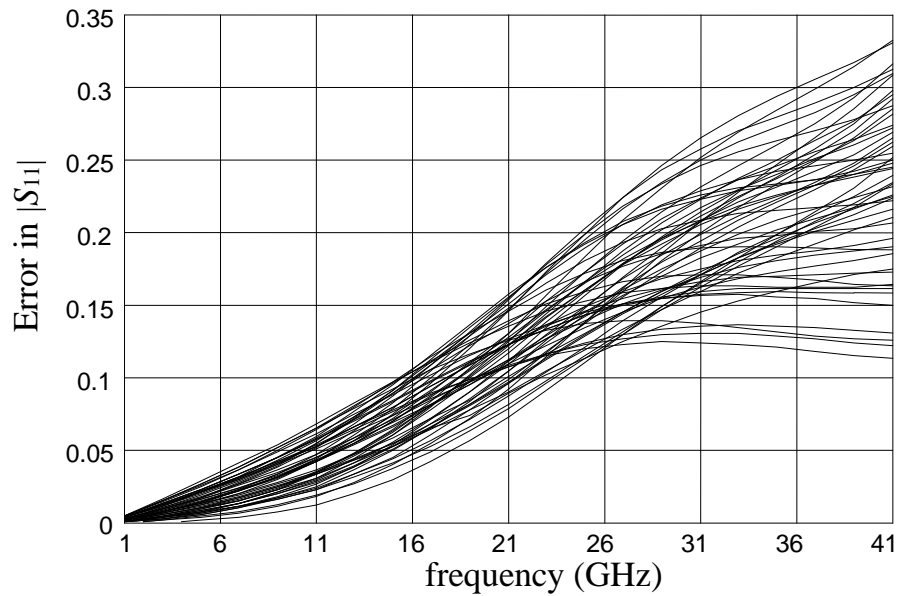
em^{TM} (o), Gupta model (●)





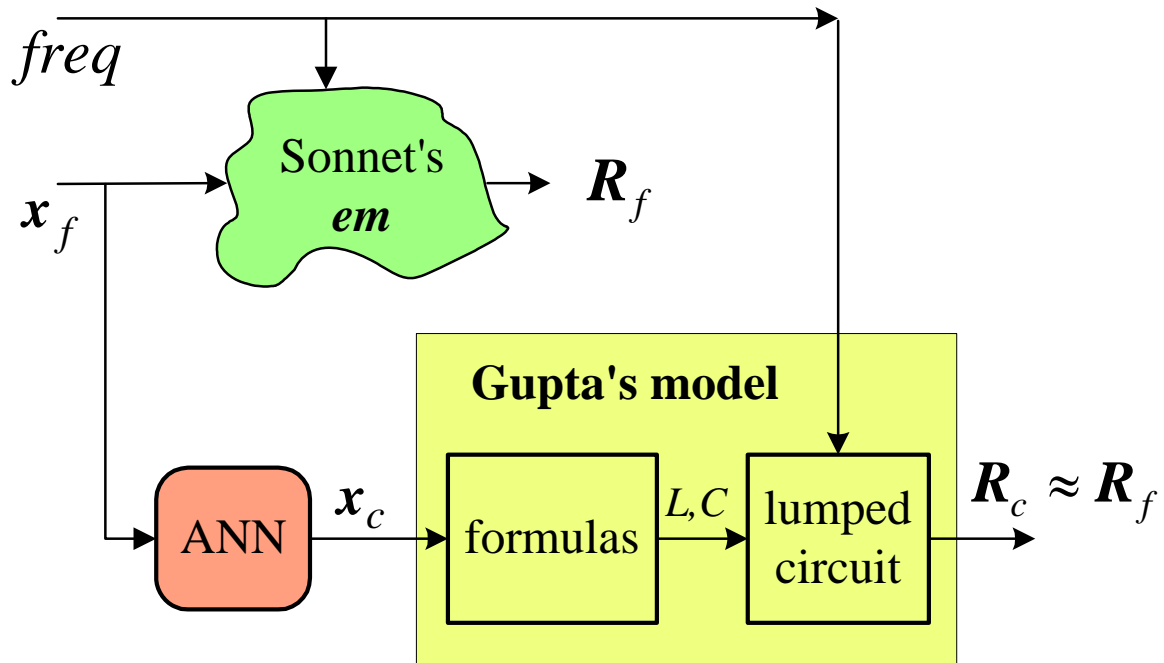
Microstrip Right Angle Bend Response Errors

comparison before neuromodeling between *em*TM and Gupta model at 50 random test points





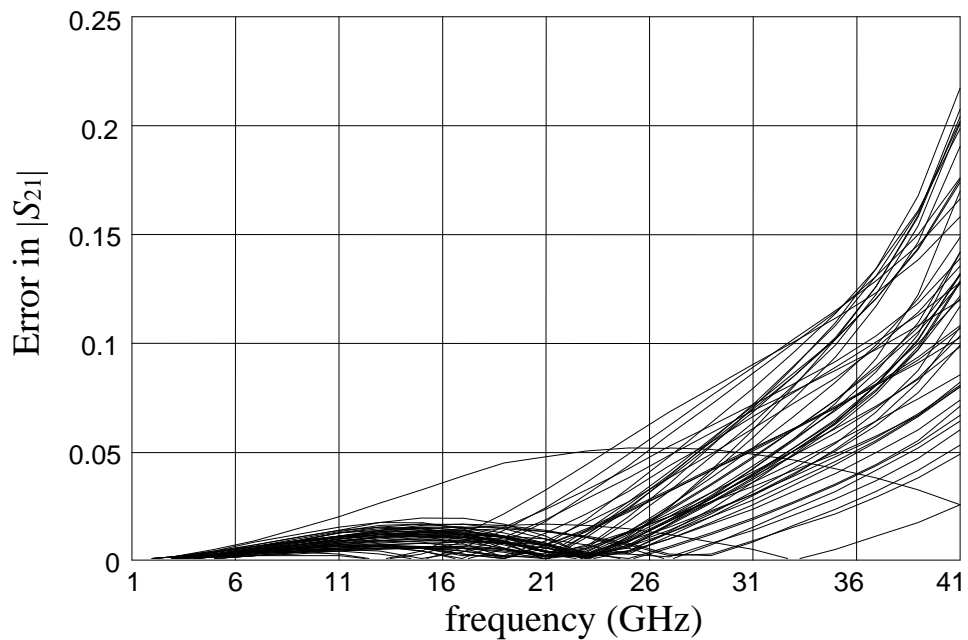
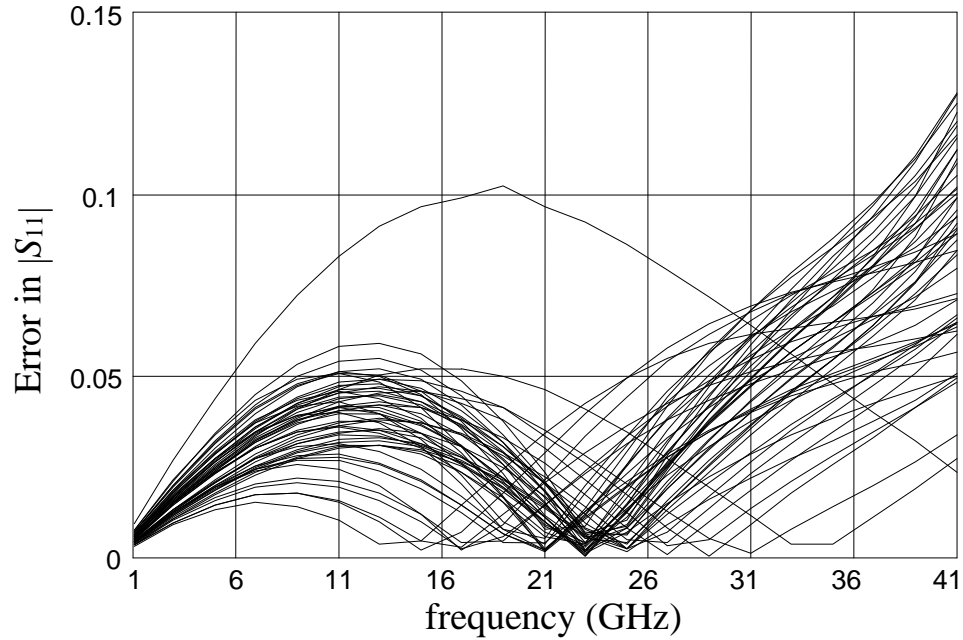
SMN Model for the Right Angle Bend (3LP:3-6-3)





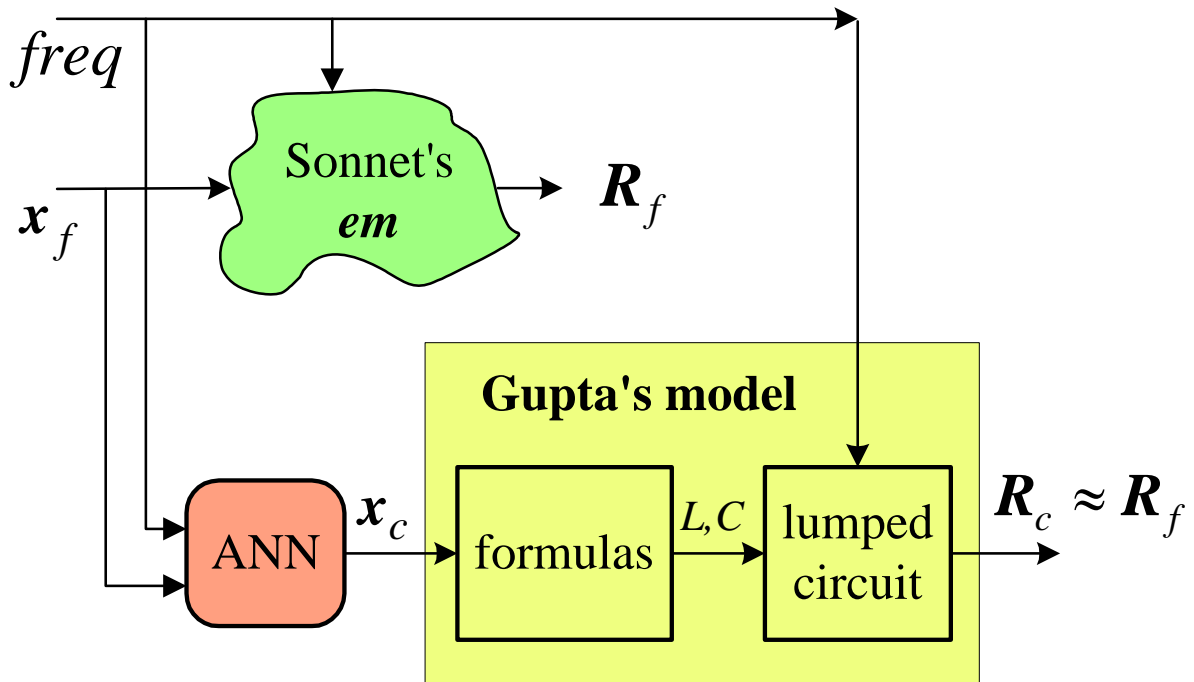
SMN Model Results for the Right Angle Bend

comparison between em^{TM} and the SMN model





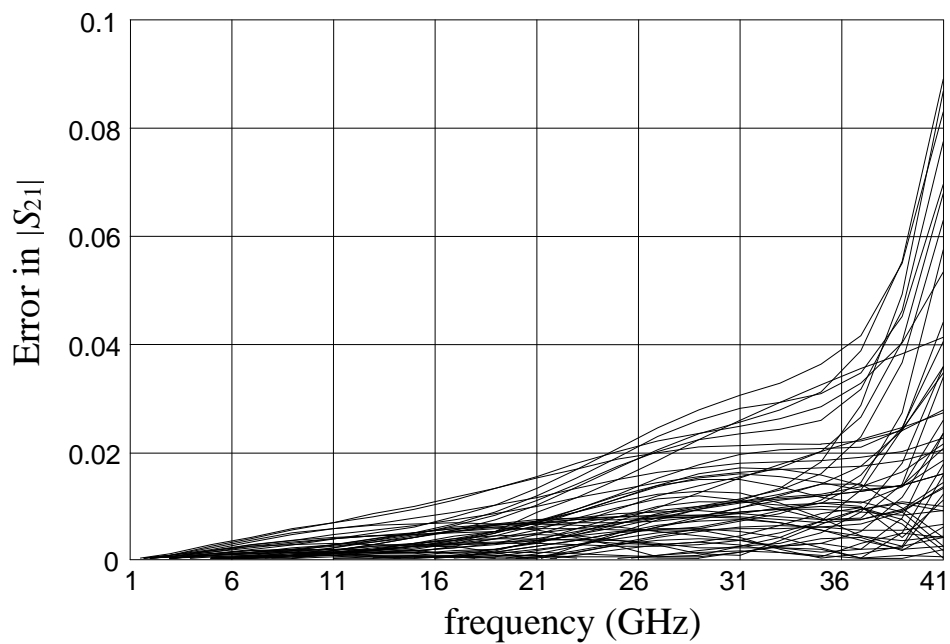
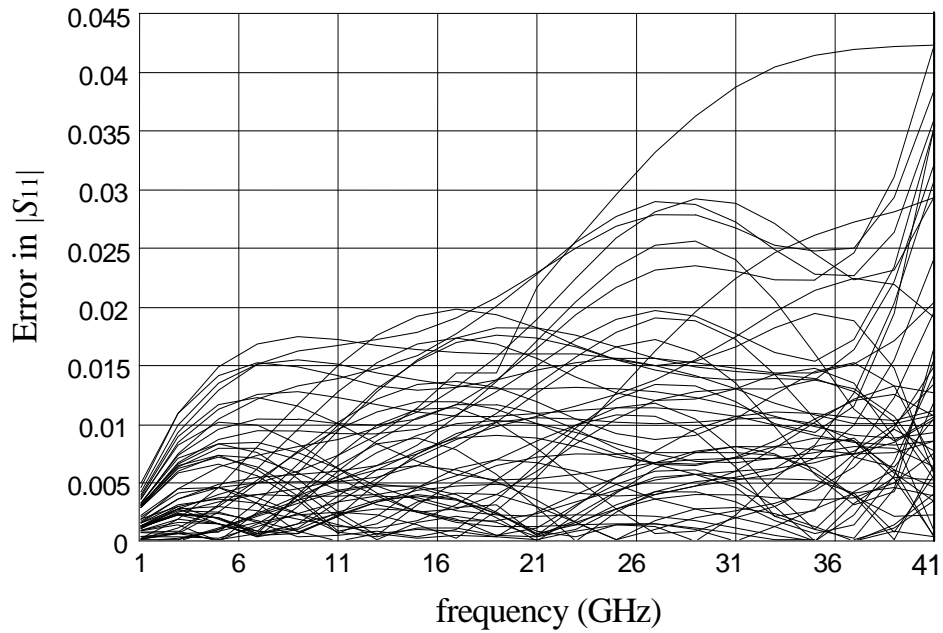
FDSMN Model for the Right Angle Bend (3LP:4-7-3)





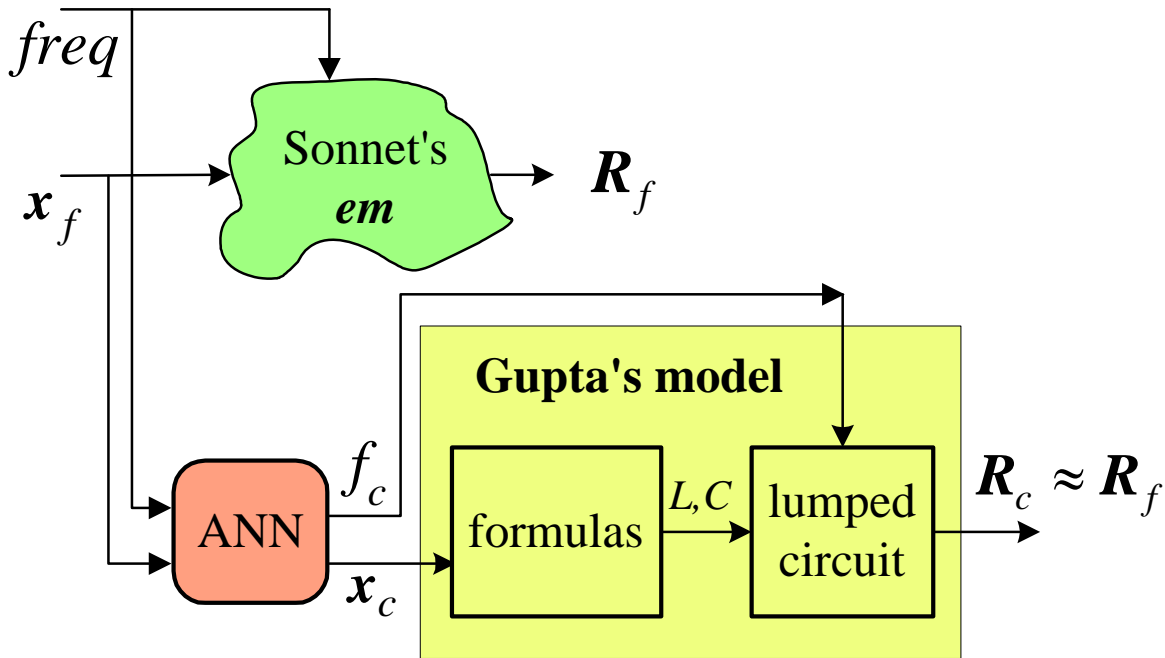
FDSMN Model Results for the Right Angle Bend

comparison between *em*TM and the FDSMN model





FSMN Model for the Right Angle Bend (3LP:4-8-4)

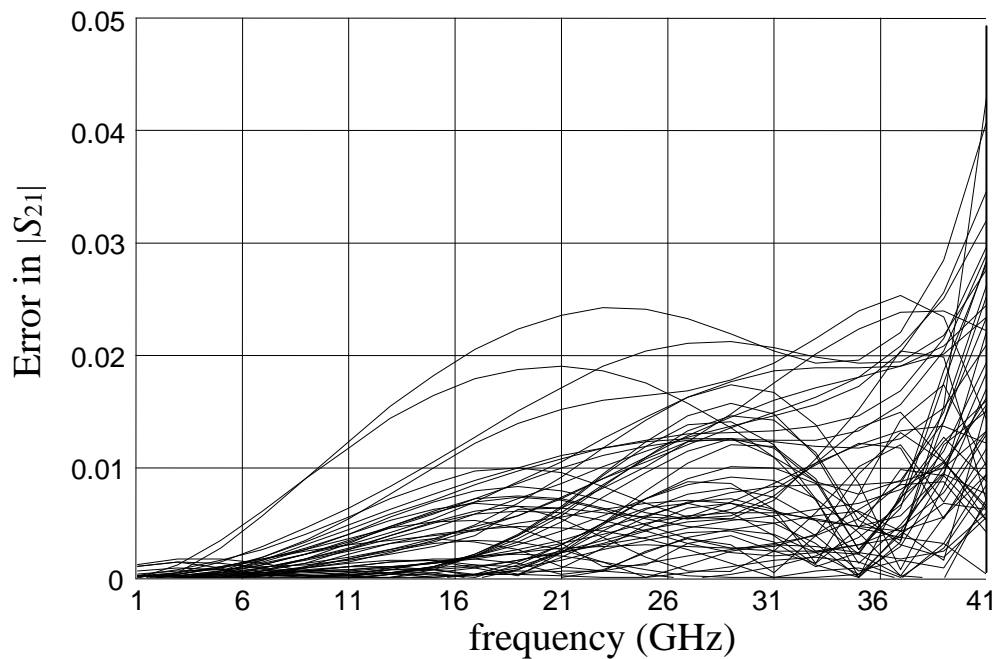
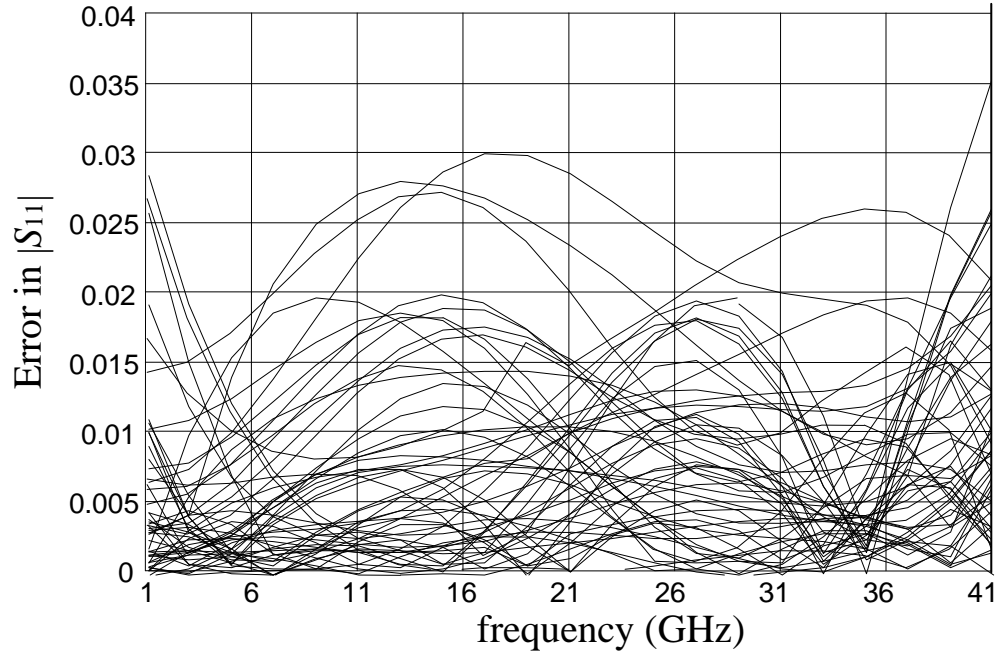


implementation: an OSA90/hope™ child program simulates the coarse model at a different frequency variable through Datapipe



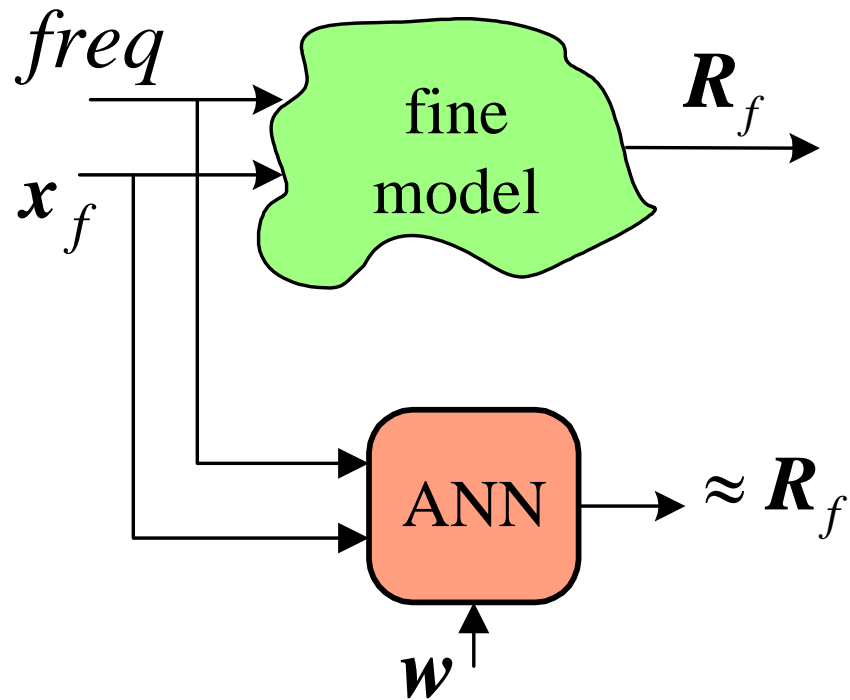
FSMN Model Results for the Right Angle Bend

comparison between em^{TM} and the FSMN model





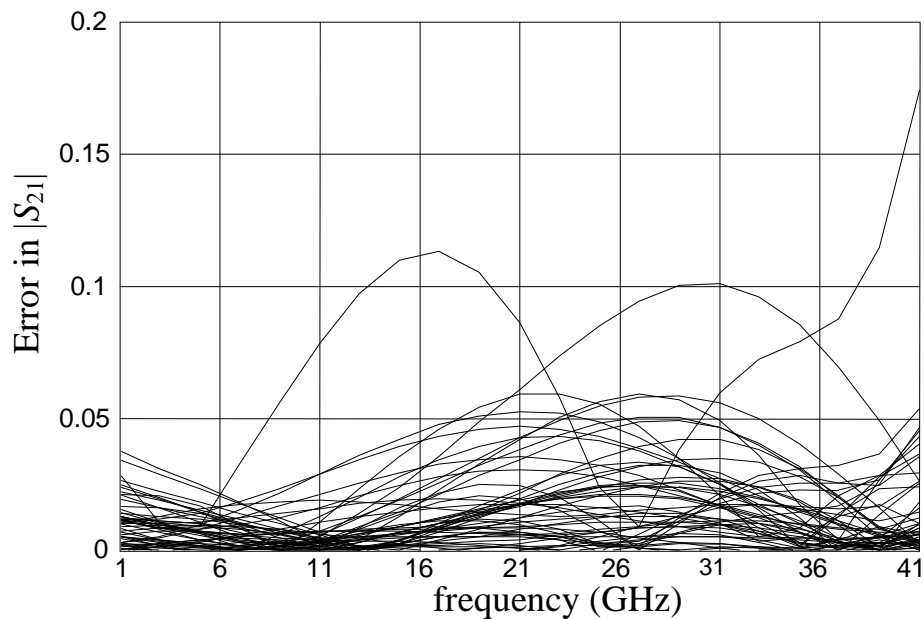
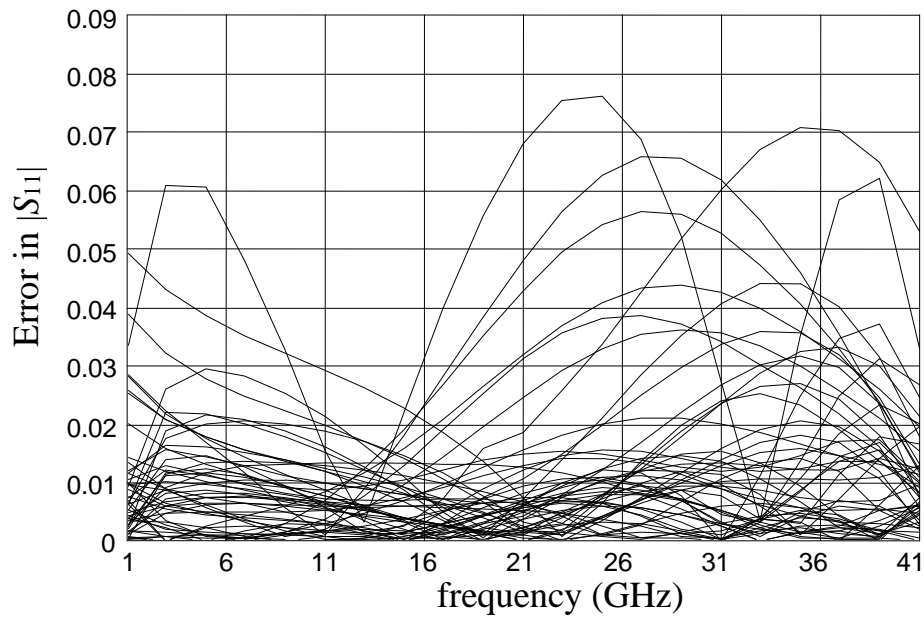
Classical Neuromodel for the Right Angle Bend (3LP:4-15-4)





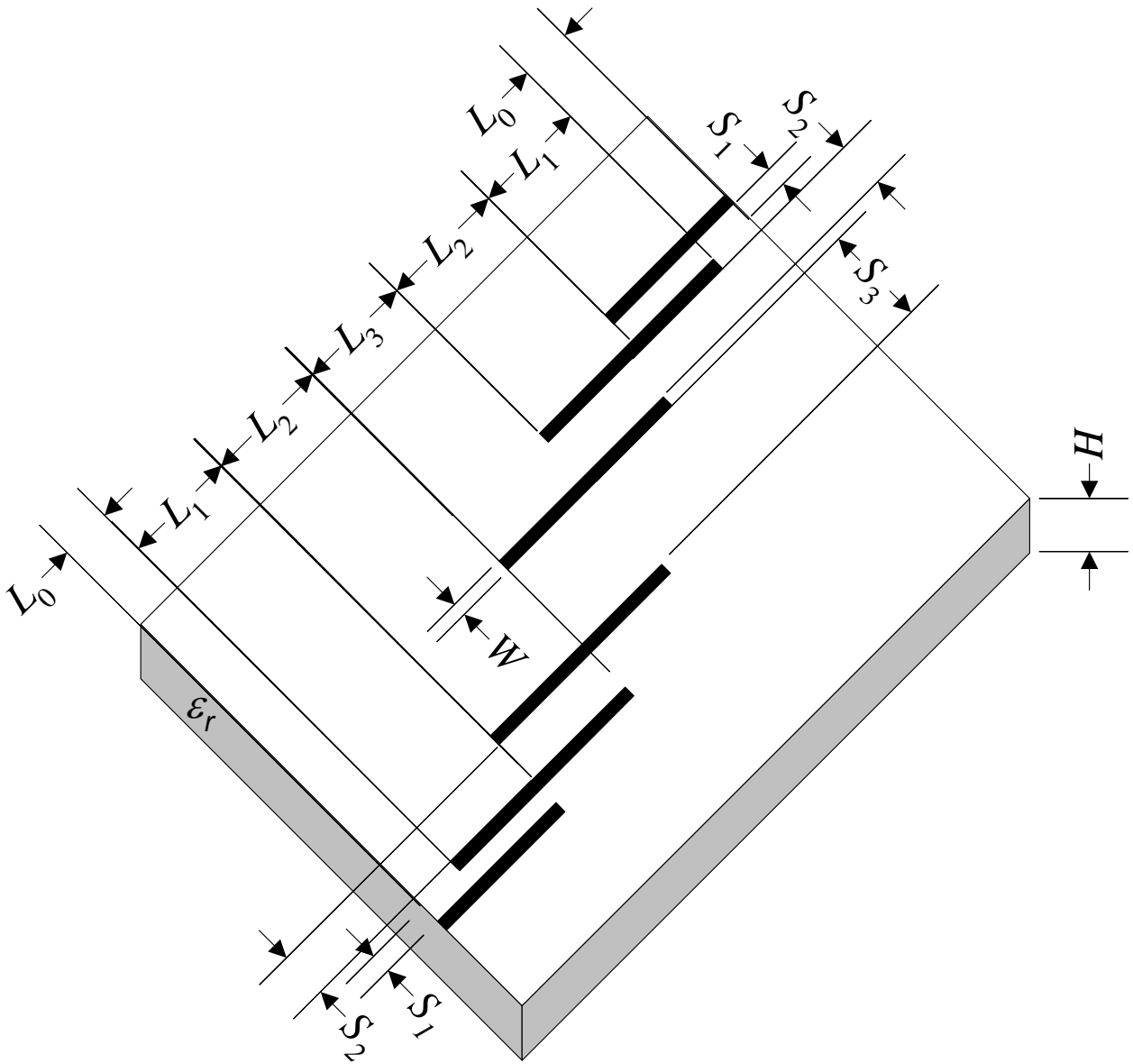
Classical Neuromodel Results for the Right Angle Bend (*Neuromodeler*, 1998)

comparison between *em*TM and classical neuromodel





HTS Quarter-Wave Parallel Coupled-Line Microstrip Filter (Westinghouse, 1993)





SM Based Neuromodeling of the HTS Filter

(Bandler *et al.*, 1999)

region of interest

$$175\text{mil} \leq L_1 \leq 185\text{mil}$$

$$190\text{mil} \leq L_2 \leq 210\text{mil}$$

$$175\text{mil} \leq L_3 \leq 185\text{mil}$$

$$18\text{mil} \leq S_1 \leq 22\text{mil}$$

$$75\text{mil} \leq S_2 \leq 85\text{mil}$$

$$70\text{mil} \leq S_3 \leq 90\text{mil}$$

$$3.901\text{GHz} \leq \text{freq} \leq 4.161\text{GHz}$$

$$L_0 = 50\text{mil}$$

$$H = 20\text{mil}$$

$$W = 7\text{mil}$$

$$\varepsilon_r = 23.425$$

$$\text{loss tangent} = 3 \times 10^{-5}$$

“coarse” model: OSA90/hope™ empirical models

“fine” model: Sonnet’s *em*™ with high resolution grid

learning set: 13 base points with “star” distribution

testing set: 7 random base points in the region of interest (not seen in the learning set)



SM Based Neuromodeling of the HTS Filter (continued)

two new SM based neuromodeling techniques have been developed; they make even better use of the implicit knowledge of the coarse model

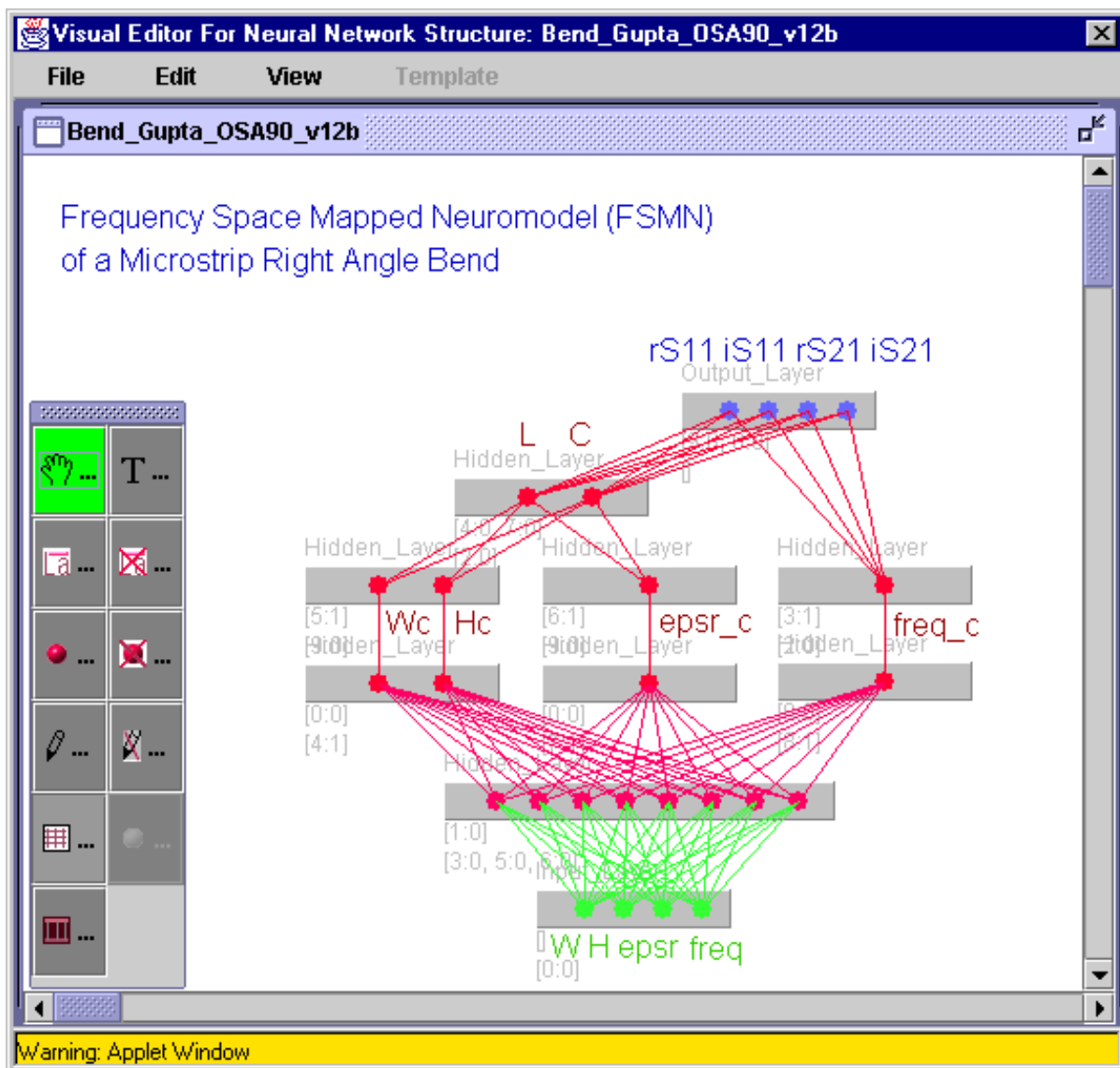
these techniques were applied to the HTS filter, with excellent results



New Realizations in NeuroModeler

SM based neuromodels of several microstrip circuits have been developed using NeuroModeler Version 1.2b (1999)

they are entered into HP ADS Version 1.1 (1999) as library components through an ADS plugin module





Conclusions

we present novel applications of Space Mapping technology to the neuromodeling of microwave circuits

three powerful techniques to generate SM based neuromodels are described and illustrated: SMN, FDSMN and FSMN

OSA90/hope™ implementations are illustrated

frequency-sensitive neuromappings expand the usefulness of quasi-static empirical models

additionally, two new SM based neuromodeling techniques have been developed; they make even more efficient use of the implicit knowledge of the coarse model (*Bandler et al., 1999*)

Huber optimization efficiently trains the neuromappings, exploiting its robust characteristics for data fitting



References

J.W. Bandler, M.A. Ismail, J.E. Rayas-Sánchez and Q.J. Zhang, "Neuromodeling of microwave circuits exploiting space mapping technology," *IEEE MTT-S Int. Microwave Symp.* (Anaheim, CA), June 1999.

P. Burrascano and M. Mongiardo, "A review of artificial neural networks applications in microwave CAD," *Int. J. RF and Microwave CAE*, Special Issue on Applications of ANN to RF and Microwave Design, vol. 9, 1999.

J.W. Bandler, R.M. Biernacki, S.H. Chen, P.A. Grobelny and R.H. Hemmers, "Space mapping technique for electromagnetic optimization," *IEEE Trans. Microwave Theory Tech.*, vol. 42, 1994, pp. 2536-2544.

H. White, A.R. Gallant, K. Hornik, M. Stinchcombe and J. Wooldrige, *Artificial Neural Networks: Approximation and Learning Theory*. Oxford, UK: Blackwell, 1992.

A.H. Zaabab, Q.J. Zhang and M.S. Nakhla, "A neural network modeling approach to circuit optimization and statistical design," *IEEE Trans. Microwave Theory Tech.*, vol. 43, 1995, pp. 1349-1358.

P. Burrascano, M. Dionigi, C. Fancelli and M. Mongiardo, "A neural network model for CAD and optimization of microwave filters," *IEEE MTT-S Int. Microwave Symp. Dig.* (Baltimore, MD), 1998, pp. 13-16.

P. Watson and K.C. Gupta, "EM-ANN models for microstrip vias and interconnects in multilayer circuits," *IEEE Trans. Microwave Theory Tech.*, vol. 44, 1996, pp. 2495-2503.

F. Wang and Q.J. Zhang, "Knowledge based neuromodels for microwave design," *IEEE Trans. Microwave Theory Tech.*, vol. 45, 1997, pp. 2333-2343.

M. Pozar, *Microwave Engineering*. Amherst, MA: John Wiley and Sons, 1998.

K.C. Gupta, R. Garg and I.J. Bahl, *Microstrip Lines and Slotlines*. Dedham, MA: Artech House, 1979.

R.M. Biernacki, J.W. Bandler, J. Song and Q.J. Zhang, "Efficient quadratic approximation for statistical design," *IEEE Trans. Circuit Syst.*, vol. 36, 1989, pp. 1449-1454.

OSA90/hope™ Version 4.0, formerly Optimization Systems Associates Inc., P.O. Box 8083, Dundas, Ontario, Canada L9H 5E7, 1997, now HP EEsof Division, Hewlett-Packard Company, 1400 Fountaingrove Parkway, Santa Rosa, CA 95403-1799.



References (continued)

*em*TM Version 4.0b, Sonnet Software, Inc., 1020 Seventh North Street, Suite 210, Liverpool, NY 13088, 1997.

EmpipeTM Version 4.0, formerly Optimization Systems Associates Inc., P.O. Box 8083, Dundas, Ontario, Canada L9H 5E7, 1997, now HP EEsof Division, Hewlett-Packard Company, 1400 Fountaingrove Parkway Santa Rosa, CA 95403-1799.

J.W. Bandler, S.H. Chen, R.M. Biernacki, L. Gao, K. Madsen and H. Yu, "Huber optimization of circuits: a robust approach," *IEEE Trans. Microwave Theory Tech.*, vol. 41, 1993, pp. 2279-2287.

NeuroModeler Version 1.0, Prof. Q.J. Zhang, Dept. of Electronics, Carleton University, 1125 Colonel By Drive, Ottawa, Ontario, Canada, K1S 5B6, 1998.

J.W. Bandler, R.M. Biernacki, S.H. Chen, W.J. Getsinger, P.A. Grobelny, C. Moskowitz and S.H. Talisa, "Electromagnetic design of high-temperature superconducting microwave filters," *Int. J. Microwave and Millimeter-Wave CAE*, vol. 5, 1995, pp. 331-343.